Compensation of nonlinearity in a fiber-optic transmission system using frequency-degenerate phase conjugation through counter-propagating dual pump FWM in a semiconductor optical amplifier

Compensation of nonlinearity in a fiber-optic transmission system using frequency-degenerate phase conjugation through counter-propagating dual pump FWM in a semiconductor optical amplifier

Abhishek Anchal[1], Pradeep Kumar K[2], Sean O'Duill[3], Prince M Anandarajah[3] and Pascal Landais[3]

[1] Department of Applied Physics, The Rachel and Selim Benin School of Computer Science and Engineering, The Hebrew University of Jerusalem, Jerusalem 90401, Israel
[2] Department of Electrical Engineering, Indian Institute of Technology Kanpur, Kanpur 208016, India
[3] School of Electronic Engineering, Dublin City University, Glasnevin, Dublin 9, Ireland

Abstract

We present a scheme of frequency-degenerate mid-span spectral inversion (MSSI) for nonlinearity compensation in fiber-optic transmission systems. The spectral inversion is obtained by using counter-propagating dual pump four-wave mixing in a semiconductor optical amplifier (SOA). Frequency-degeneracy between signal and conjugate is achieved by keeping two pump frequencies symmetrical about the signal frequency. We simulate the performance of MSSI for nonlinearity compensation by scrutinizing the improvement of the Q-factor of a 200 Gbps QPSK signal transmitted over a standard single mode fiber, as a function of launch power for different span lengths and number of spans. We demonstrate a 7.5 dB improvement in the input power dynamic range and an almost 83% increase in the transmission length for optimum MSSI parameters of −2 dBm pump power and 400 mA SOA current.

Keywords: non-linearity compensation, optical phase conjugation, semiconductor optical amplifier, four-wave mixing, non-linear optics

1. Introduction

Technological development in recent years has created the high-speed data network, which currently serves as the backbone to cater for the increasing demand of bandwidth-rich applications such as online gaming, video sharing and streaming, voice over Internet, video on demand, and cloud computing. Such services are bandwidth intensive, pushing the capacity of network providers to their transmission limit [1, 2]. Cisco VNI predicts that there will be a five- to seven-fold increase in the global data traffic (of the order of zettabytes) between 2016 and 2021 [3]. The advancement with wavelength division multiplexing (WDM), higher-order modulation formats such as quadrature phase shift keying (QPSK), quadrature amplitude modulation (QAM), coherent detection, and space diversity make fiber optic transmission system a true candidate to support high capacity network in the present scenario as well as in the near future context [4–7]. The capacity can be further enhanced by using a superchannel with several sub-carriers separated by a smaller channel spacing [8]. However, the capacity of fiber-optic transmission systems is limited by distortion due to fiber

nonlinearities resulting from large launched powers for higher modulation formats and/or small channel spacing [2, 4, 5, 9–11]. Therefore, recent research have been focused on reducing the effect of fiber nonlinearities through various compensation techniques, such as phase-conjugated twin wave, optical back-propagation, digital nonlinearities compensation, nonlinear Fourier transform, mid-span spectral inversion (MSSI) and so on [10–15].

Among these techniques, MSSI using optical phase conjugation (OPC) has been shown to fully compensate for the distortion due to fiber nonlinearities, in intensity and phase modulated systems [11, 16, 17]. Other advantages of using MSSI are: transparency to modulation formats, scalability in WDM systems, and implementation in the optical domain to take advantage of the underlying optical fiber infrastructure. MSSI using OPC was first demonstrated in [18], in which the distortion due to fiber dispersion and nonlinearities in the first half of the transmission link is inverted by OPC and canceled by similar distortion in the second half of the transmission link. As the effect of fiber dispersion in higher modulation formats is less than the legacy on-off-keyed systems, various MSSI schemes have been reported to compensate for fiber nonlinearities, including OPC based on three-wave mixing in a lithium niobate crystal and four-wave mixing (FWM) in highly nonlinear fiber (HNLF), semiconductor optical amplifier (SOA), and silicon waveguide [16, 17, 19, 20, 21]. However, frequency conversion during the OPC process results in a crosstalk in WDM system causing bit-errors and hence resulting in a reduction in the overall improvement in capacity of the transmission system. There have been various attempts to generate frequency-degenerate MSSI using dual pump orthogonally polarized co-propagating FWM in fibers or SOAs [22, 23]. These techniques require the signal to be co- and orthogonally-polarized with respect to the two pumps and result in an orthogonally-polarized conjugate with respect to the signal. Since the polarization of the signal cannot be readily controlled in a transmission system, both frequency and polarization shift free MSSI is required.

In this paper, we utilize our previously reported method of frequency and polarization shift free OPC (FS-OPC) in SOA [24] as MSSI, for nonlinearities compensation of a 200 Gbps QPSK modulated signal transmitted over 800 km–1200 km standard single mode fiber (SSMF). High nonlinearities, excellent phase-matching with short active lengths (500 μm–2000 μm), small pump power requirements due to inherent amplification, and easier photonic integration makes SOA a better candidate for MSSI than HNLF [25]. Hence, we discuss MSSI using FS-OPC by a counter-propagating dual pump FWM in an SOA. The two counter-propagating pumps are input at the opposite ends of the SOA and a signal co-propagating with one of the pumps is input to the SOA. The beating between the co-propagating pump and the signal creates a refractive index and gain grating in the active layer of the SOA. The other pump diffracts from the grating to generate a phase-conjugate version of the signal. The signal and its conjugate appear at opposite ends of the SOA [24]. A frequency shift between the signal and its conjugate is avoided by keeping the two pump frequencies symmetrical about the signal frequency, while polarization-shift is avoided by keeping the two pumps co-polarized [26]. It is important to note that the MSSI can compensate for fiber nonlinearities in QAM and other higher modulation formats [27]. However, we considered the nonlinearities compensation of QPSK modulated signal, to reduce the computational complexity.

We investigate the performance of MSSI for nonlinearities compensation, by studying the Q-factor of a 200 Gbps QPSK signal received with and without MSSI as a function of launched signal power for various span lengths and number of spans. Further, we study the performance dependence of MSSI on the parameters, namely, pump power and SOA current. The results achieved show that a 7.5 dB increase in input power dynamic range (IPDR) and an 83% improvement in transmission length can be obtained.

The rest of the paper is organized as follows: in section 2, we present our MSSI scheme using FS-OPC by counter-propagating dual pump FWM in an SOA. In section 3, we carry out numerical simulations to scrutinize the performance of MSSI as nonlinearities compensation of a QPSK signal by studying the Q-factor variation as a function of launched power for different span lengths and number of spans. We also investigate the performance dependence of MSSI on pump power and SOA current. Finally, in section 4, we conclude by summarizing the results.

2. System description

Figure 1 shows the schematic diagram of a transmission link containing the frequency-degenerate MSSI using FS-OPC. The optical carrier of angular frequency ω_s from a laser diode is QPSK modulated with symbols $b_n \in \{1, +j, -1, -j\}$ and launched into the first half of the transmission link. The signal is distorted by dispersion and nonlinearities induced phase in $n \times L$ km of SSMF. This distorted phase is inverted by MSSI placed at the middle of the link as shown in figure 1. The phase-inverted signal propagates through the second half of the link (of SSMF length $n \times L$), where the signal experiences similar distortions as those experienced in the first half, in such a way the new distortions cancel out the inverted distortion. Subsequently, the received signal is coherently detected and original transmitted symbols are recovered. The Q-factor (in dB) is obtained by counting the bit-error rate (BER) from the detected sequence, using

$$Q = 20 \times \log_{10}(\sqrt{2} \times \mathrm{erfc}^{-1}(2\mathrm{BER})). \quad (1)$$

We include dispersion compensating fibre (DCF), so we can focus on the compensation of the fibre non-linearities by MSSI. Although, MSSI has proven to compensate for dispersion [18].

The frequency-degenerate MSSI using counter-propagating dual pump FWM in an SOA is shown in the inset of figure 1. The signal power is reduced by an attenuator (to avoid operating the SOA in a saturation regime), then combined with pump$_1$ (at angular frequency ω_1) and injected into the SOA from port 1. Pump$_2$ (at angular frequency ω_2) is

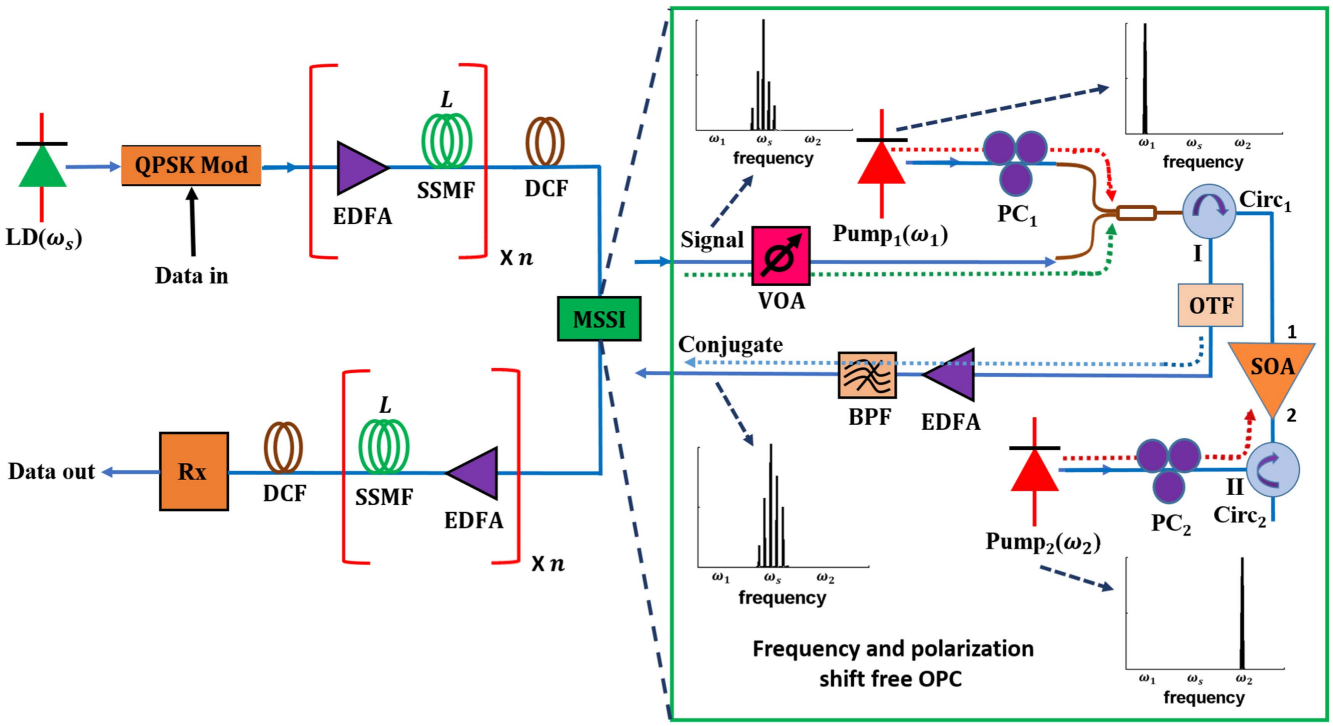

Figure 1. Simulation setup to study nonlinearity compensation of QPSK signal transmission through n span of L km SSMF using frequency-degenerate MSSI through counter-propagating dual pumped FWM in SOA. LD = laser diode, QPSK Mod = quadrature phase-shift keying modulator, EDFA = erbium doped fiber amplifier, SSMF = standard single mode fiber, DCF = dispersion compensating fiber, $PC_{1,2}$ = polarization controller, VOA = variable optical attenuator, $Circ_{1,2}$ = circulator, SOA = semiconductor optical amplifier, OTF = optical tunable filter, BPF = band pass filter, Rx = receiver.

injected from port 2. The pump frequencies are kept symmetrical about the signal frequency as shown in the spectra of figure 1. The beating between signal and $pump_1$ leads to a refractive index and gain grating inside the active layer of the SOA, which diffracts the $pump_2$ to create a conjugate copy of the signal (with inverted spectrum at the central frequency ω_s) propagating in the opposite direction of the signal [24, 28]. Polarization controllers ($PC_{1,2}$) are used to keep the two pumps co-polarized, to obtain a higher conjugate efficiency. In a recent study, we have demonstrated an OPC efficiency of 1% with an SOA [24]. The conjugated signal is filtered from the co-propagating $pump_2$ by an optical tunable filter and amplified by an EDFA before being transmitted in the second half of the network. A band pass filter removes the noise introduced by the EDFA.

Expression for phase-conjugation

We obtain the equations governing the evolution of signal and conjugate by solving the nonlinear Schrödinger equation with a total electric field inside the SOA, $\sum_{i=1,2}E_i(z,t)\exp(j(\omega_i t + (-1)^i k_i z)) + E_s(z,t)\exp(j(\omega_s t - k_s z)) + E_c(z,t)\exp(j(\omega_s t + k_s z))$ and assuming the gain saturation is dominated by two pumps, as [28],

$$\frac{\partial E_s}{\partial z} = -\mu_s E_s + j\upsilon_s E_c^* \exp(j\Delta k z)$$
$$\frac{\partial E_c^*}{\partial z} = \mu_c^* E_c^* + j\upsilon_c^* E_s \exp(-j\Delta k z) \quad (2)$$

where E_m, $m = 1, 2, s, c$ are the electric field envelopes of $pump_1$, $pump_2$, signal, and conjugate respectively, $\Delta k = k_1 - k_2$, k_n, $n = 1, 2, s$ are propagation constant of $pump_1$, $pump_2$, and signal, respectively, and $\mu_{s,c}$ and $\upsilon_{s,c}$ are given by

$$\mu_{s,c} = -\frac{g_0}{2(1+P_0)}\left[1 - j\beta - \frac{\omega^2}{\Delta\omega_g^2} - \frac{(1-j\bar{\beta})CrP_0}{1 \mp j\Omega T_2/2}\right] + \frac{g_0}{2(1+P_0)}\frac{(1-j\bar{\beta})CrP_0}{1 \mp j\Omega T_2/2}\frac{1}{1 \mp j\Omega T_1}$$
$$\upsilon_{s,c} = \frac{jg_0}{2(1+P_0)}\frac{Cr[1 - j\bar{\beta}(1 \mp j\Omega T_2)]}{(1 \mp j\Omega T_2)(1 \mp j\Omega T_1)}2E_1E_2 \quad (3)$$

where $-$ and $+$ sign goes for s and c respectively Ω is the detuning between the pump and the signal, $g_0 = \Gamma a \bar{N}_0 (I/I_0 - 1)$ is the small signal gain, Γ denotes the confinement factor, a ($\simeq 2 \times 10^{-16}$ to 3×10^{-16} cm^2) the gain coefficient, and I is the SOA current. I_0 is the current needed to achieve transparency in the active region of the SOA, $\bar{N}_0$ ($\simeq 1 \times 10^{18}$ to 2×10^{18} cm^{-3}) is the carrier density at I_0, β ($\simeq 3$ to 6) is the linewidth enhancement factor, and P_0 is the intra-cavity pump power. Other parameters are given in [28]. Equation (2) is valid for a large pump-signal detuning exceeding 100 GHz [28]. The expression for a phase-conjugated signal is obtained by solving (2) subjected to boundary conditions:

$E_s(z=0) = E_{s0}$ and $E_c(z = L_{SOA}) = 0$,

$$E_c(z) = -j\upsilon_c E_{s0}^* e^{-(\chi^* - \mu_c)z} \times \left[\frac{\sin\zeta(L_{\mathrm{SOA}} + z)}{\chi\sin\zeta L_{\mathrm{SOA}} + \zeta\cos\zeta L_{\mathrm{SOA}}}\right]^* \quad (4)$$

where $\chi = (\mu_s + \mu_c^* + \Delta k)/2$ and $\zeta = \sqrt{(2\chi)^2 - \upsilon_s\upsilon_c^*}/2$. Thus, at $z = 0$, E_c is a phase-conjugate of the input signal E_{s0} with an additional phase-constant. It is interesting to note that the perfect phase-conjugation is possible with a similar scheme using HNLF as reported in our previous work [26]. We see that, at $z = 0$, conjugate ($E_c(0)$) and conjugate efficiency $\left(\frac{|E_c(0)|^2}{|E_{s0}|^2}\right)$ depend upon the pump power and the SOA current through χ and ζ. Therefore, the MSSI transmission performance is dependent on these two as well.

3. Performance of SOA-based MSSI

We investigate the performance of MSSI by numerically simulating the scheme shown in figure 1, by evaluating the Q-factor of a 200 Gbps QPSK transmission system with and without MSSI. For the sake of simplicity, we only consider a single polarization QPSK transmission system. The length (L) of SSMF ($\alpha = 0.2$ dB/km, $D = 16$ ps/nm-km) is taken as 80 km and the total number of spans ($2n$) as 10 throughout the simulation unless otherwise specified. The parameters for DCF are: $\alpha_{dcf} = 0.5$ dB/km and $D = -80$ ps/nm-km and length of DCF are chosen to compensate the dispersion in the SSMF, whereas the parameters of the EDFA are taken as: gain = 30 dB and noise-figure = 5 dB. The wavelengths of the signal, pump$_1$, and pump$_2$ are 1550 nm, 1550.8 nm, and 1549.2 nm, respectively. The linewidth of the signal and the pump waves are taken as 100 kHz and 10 kHz, respectively, whereas the optical signal to noise ratio (OSNR) of the signal and the pump waves is kept at 40 dB and 60 dB, respectively. Parameters of the SOA are: $\beta = 4$, $\Gamma = 0.5$, $L_{SOA} = 1$ mm, $\bar{N}_0 = 2 \times 10^{18}$ cm^{-3}, $a = 3 \times 10^{-16}$ cm^2. We use a MATLAB-based simulation toolbox Optilux to simulate the transmission system [29].

We simulate a 200 Gbps QPSK transmission system with and without MSSI for total transmission distance of 1600 km to understand the impact of MSSI. Figures 2(a) and (b) show the eye-diagram of the received signal with and without MSSI, respectively. In figure 2(a), a nearly complete eye closure of the transmitted signal can be seen. It can be ascribed to signal distortion due to fiber nonlinearities, while in figure 2(b), the effect of the nonlinearities compensation by the MSSI can be observed validated by the wide open eye with respect to the previous eye.

3.1. Q-factor versus launched power with increased span length

We simulate a 200 Gbps QPSK transmission system with and without MSSI as a function of launched signal power for different span lengths but with a number of spans (n) set to 10. Pump power and SOA current are kept at -2 dBm and 400 mA, respectively, to avoid saturation of the SOA.

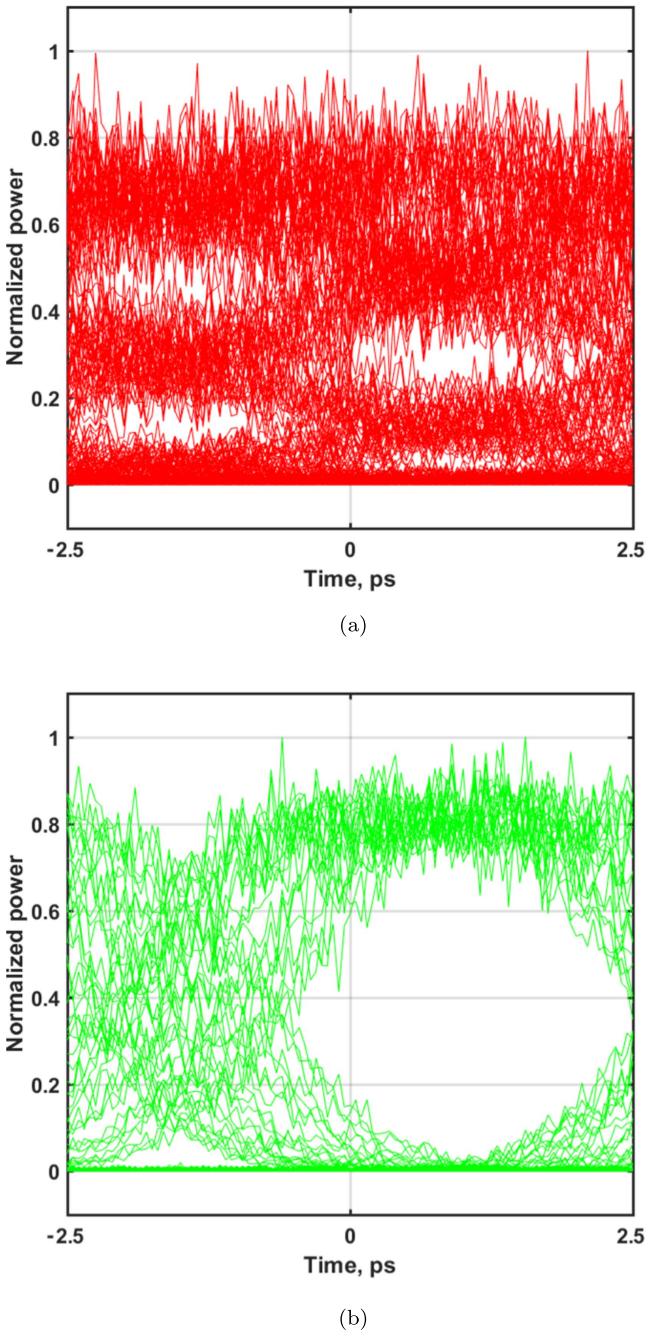

Figure 2. Eye diagram of 200 Gbps received signal (a) with and (b) without MSSI. Span length, total number of spans, and SOA current are kept at 80 km, 20, and 400 mA, respectively.

Figure 3(a) shows the simulation results of Q-factor versus launch power for increased span length (80 km: ×, 100 km: ◊, 120 km: □). All red lines show Q-factors for the reference system without MSSI, whereas all green lines represent the Q-factors for the transmission system with MSSI. The black dashed (–) line shows the FEC limit corresponding to a BER of 4×10^{-3} [30]. The Q-factor increases with launch power due to an increase in the OSNR and then decreases due to an increase in SSMF nonlinearities

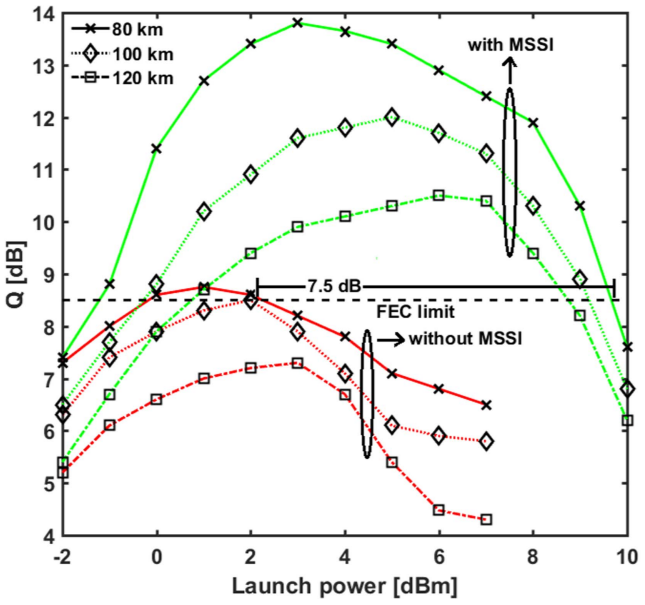

(a)

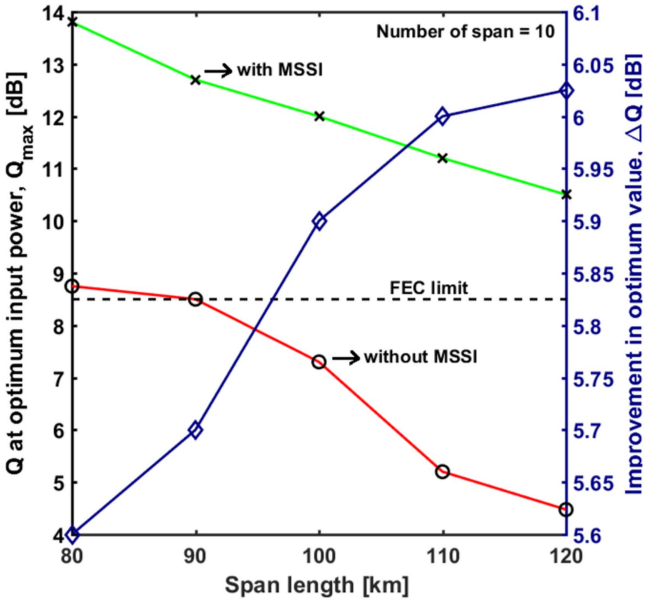

(b)

Figure 3. (a) Q-factor versus launch power with and without MSSI for 200 Gbps QPSK transmission with different span lengths (80 km, 90 km, and 120 km). (b) Optimum Q-factor and improvement versus span length. The total number of span, pump power, and SOA current are 10, −2 dBm, and 400 mA, respectively.

at higher launched powers. There is an improvement of Q-factor when MSSI is deployed in the reference system. As the launched power increases, the improvement in the Q-factor augments due to an increase in the conjugate-efficiency. However, at launch powers higher than 8 dBm the Q-factors decreases sharply and falls below the forward error correction (FEC) limit. This is due to the saturation of the SOA at higher powers. The maximum Q-factor of 13.8 dB is obtained at an optimum launched power of 3 dBm for a system with a span length of 80 km and the improvement in Q-factor at this optimum launched power is 5.6 dB. Further, we observe the IPDR spanning from 2 dBm to 9.5 dBm with a total improvement of 7.5 dB, when MSSI is used with a 10 × 80 km transmission reach.

The maximum span length of the reference system is 80 km, after which the Q-factor degrades below the FEC limit. On the other hand, the transmission system with MSSI sustains its Q-factor above the FEC limit up to 120 km of span length. Therefore, the total transmission length is increased from 10 × 80 km to 10 × 120 km. Figure 3(b) shows a maximum Q-factor for span lengths of 80 km to 120 km for a transmission system with (green line with ×) and without (red line with ○) MSSI and a corresponding improvement in Q-factor with MSSI (blue line with ◊). The increase in span length causes the increase in nonlinear power asymmetry in the two halves of the transmission fiber resulting in less efficient functioning of MSSI, leading to a degradation of the Q-factor. However, the improvement in ΔQ with an increase in span length suggests that the effect of nonlinearities compensation due to MSSI extends the span length. This is due to an improvement in the maximum permissible launched power when MSSI is used.

With a BER set at 10^{-3}, we observe a IPDR between −1 dBm and 10 dBm, between 0 dBm and 9.5 dBm, and between 1 dBm and 9 dBm for the span lengths 80 km, 100 km, and 120 km, respectively.

Finally, we observe the improvement in Q-factors, maximum launched power, and IPDR when MSSI is used, suggesting the fiber nonlinearities compensation by MSSI. The transmission system is also able to benefit from an increase in the maximum permissible launched power to the transmission length by having a longer span. At the transmission length of 10 × 80 km, improvement in Q-factor and maximum launched power due to MSSI are 5.6 dB and 7.5 dB, respectively.

3.2. Q-factor versus launched power with increased number of span

We also investigate the improvement in Q-factor due to MSSI for a longer transmission length with an increasing number of spans and keeping span length fixed to 80 km. Figure 4(a) shows the Q-factor versus launched power for three different span numbers (10: ×, 12: ◊, 14: □) for both, a transmission system with (green lines) and without MSSI (red line). The Q-factor of the reference transmission system without MSSI falls below the FEC limit for any span number larger than 10. However, the transmission system with MSSI shows less degradation in Q-factor with increasing transmission length as the nonlinear power asymmetry on either side of MSSI becomes less and less significant with increasing number of spans (as compared to increasing transmission length by increasing span length at fixed number of span). The IPDR is between −1.2 dBm and 9.6 dBm for 10 spans, between −1 dBm and 9.5 dBm for 12 spans, and between −0.8 dBm and 9.4 dBm for 14 spans.

Figure 4(b) shows the Q-factor at the optimum input power as a function of transmission length for a system with

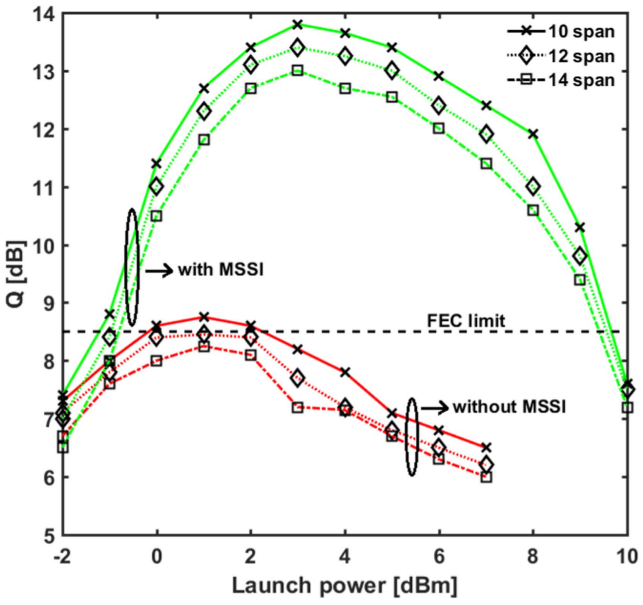

(a)

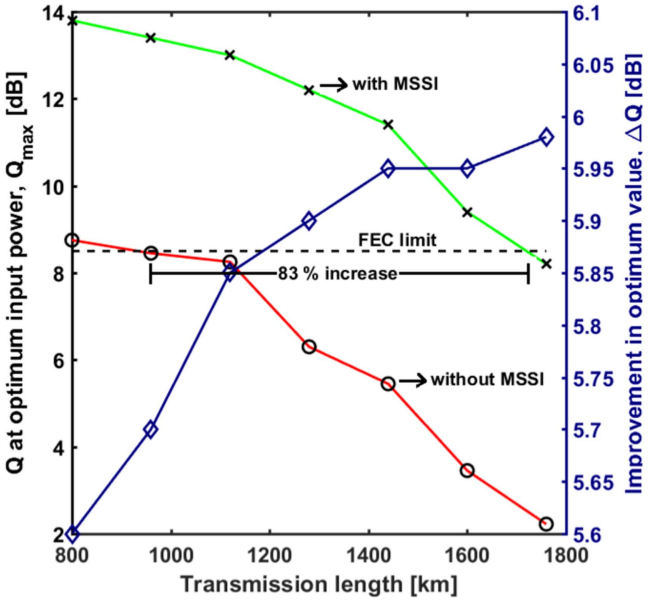

(b)

Figure 4. (a) Q-factor versus launch signal power with and without MSSI for 200 Gbps QPSK transmission with different transmission lengths (10 × 80 km, 12 × 80 km, and 14 × 80 km). (b) Optimum Q-factor and improvement versus transmission length. The span length, pump power, and SOA current are 80 km, −2 dBm, and 400 mA, respectively.

(green line with ×) and without MSSI (green line with ○). The optimum Q-factor in the reference system falls below the FEC limit after 12 × 80 km of transmission distance, while the Q-factor for the MSSI system is above the FEC limit before 22 × 80 km. This shows that SOA-based MSSI can improve the maximum transmission length by more than 83% with a span length of 80 km. The blue line with ◊ in figure 4(b) shows a 5.6 dB improvement in Q-factor when

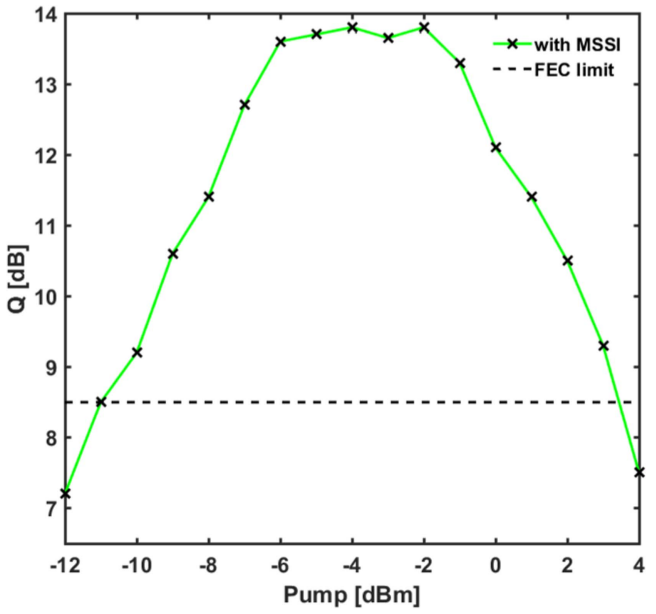

Figure 5. Q-factors dependence on SOA pump power. The FEC limit corresponds to BER of 4×10^{-3}.

MSSI is used in 10 × 80 km transmission length. Further, this improvement increases by 0.4 dB when transmission length increases from 10 × 80 km to 22 × 80 km.

Performance dependence of transmission system on MSSI parameters

We next investigate the performance dependence of MSSI for nonlinearities compensation in a transmission system on parameters of MSSI itself, by changing its control parameters, namely, pump power and SOA current.

3.3. Influence of pump power

We study the effect of pump power on the nonlinearities compensation by MSSI by simulating the Q-factor as a function of pump power for a transmission length of 10 × 80 km SSMF. The launched signal power and SOA current are kept at 3 dBm and 400 mA, respectively. Figure 5 shows the dependence of Q-factor on pump power. The solid line with a cross (×) and the dashed line (–) denotes the Q-factor with MSSI and FEC limit corresponding to BER of 4×10^{-3}, respectively. The Q-factor increases with pump power, due to an increase in the conjugate-efficiency and attains a values between 13.3 dB–13.8 dB until a pump power of −1 dBm is reached. Thereafter, Q-factors decreases with pump power and goes below the FEC limit after a pump power of 3 dBm. This is due to saturation of SOA resulting in a lower conjugate-efficiency at higher pump powers.

3.4. Q-factor versus signal power with different SOA currents

Figure 6(a) shows the Q-factor versus signal power for the reference transmission system without MSSI and the transmission system with MSSI at different SOA currents (400 mA: ×, 300 mA: ◊, 200 mA: □, 125 mA: ∗). The pump

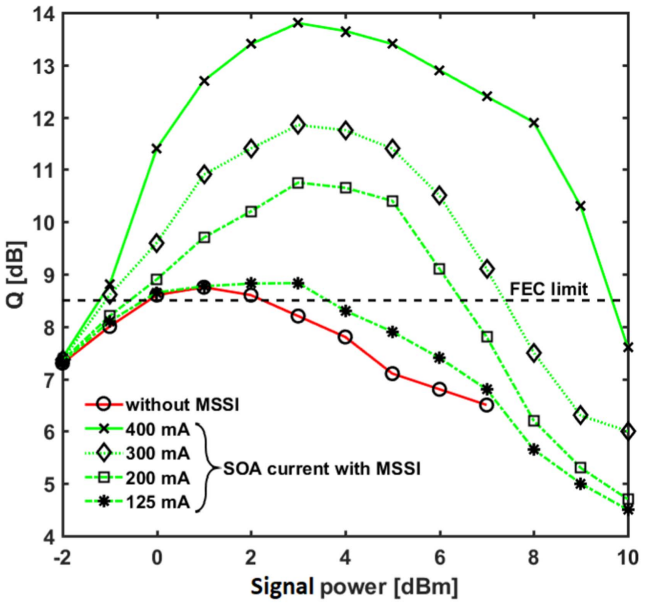

(a)

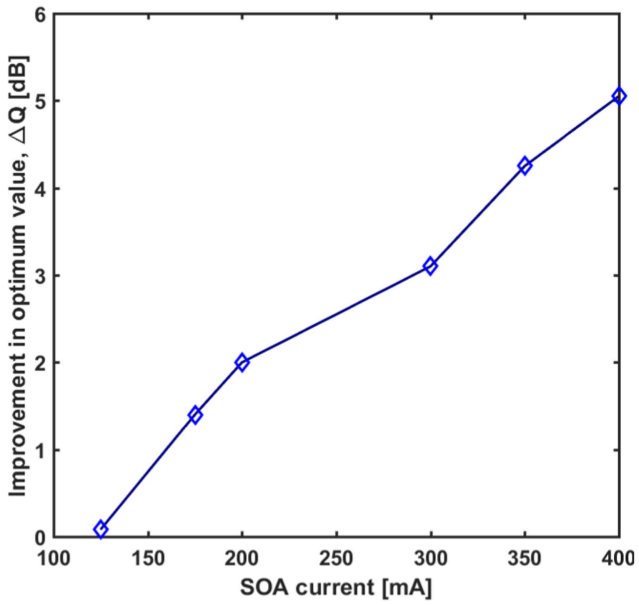

(b)

Figure 6. (a) Q-factor versus launch power with and without MSSI for 200 Gbps QPSK transmission with different SOA current (400 mA, 300 mA, 200 mA, and 125 mA). (b) Improvement in optimum Q-factor versus SOA current. The pump power, span length, and number of span are −2 dBm, 80 km, and 10, respectively.

power, span length and number of spans are kept at −2 dBm, 80 km, and 10, respectively. The green and red line show the Q-factor of the system with and without MSSI, respectively. As the SOA current increases the small signal gain (g_0) increases, which results in an increase in conjugate-efficiency and hence performance of MSSI is improved resulting in a optimum Q-factor as high as 13.8 dBm at 400 mA SOA current. Further, the improvement of MSSI performance (in nonlinearities compensation) is suggested by the enhancement of IPDR from [0 dBm–3.8 dBm] to [−1 dBm −9.7 dBm], when the SOA current is increased from 125 mA to 400 mA. Figure 6(b) shows the improvement in the optimum Q-factor when MSSI is used as a comparison to the reference system. Improvement in the optimum Q-factor increases with an increase in SOA current and an increment of 5 dB of improvement in the optimum Q-factor is obtained when the SOA current is increased from 125 mA to 400 mA.

4. Summary

We have presented a scheme of frequency-degenerate MSSI by FS-OPC through counter-propagating dual pump FWM in SOA, for nonlinearities compensation of a 200 Gbps QPSK signal transmitted over SSMF. Frequency-degeneracy between the signal and the conjugate is obtained by placing the pump frequencies symmetrical about the signal frequency. The polarization of the signal and the conjugate are maintained (co-polarized) by using two co-polarized pumps. The SOA has proven to be a device of interest in the FS-OPC scheme as it exhibits non-linear mechanisms sustaining >100 GHz pump-probe detuning.

We have examined the performance of MSSI for nonlinearities compensation of a QPSK transmitted signal by simulating the Q-factor as a function of launched power for different span lengths and number of spans. The nonlinearities compensation is visualized by an increase in Q-factor by 5.6 dB at 3 dBm launched power for transmission length of 10 × 80 km, when MSSI is used. We also observed the improvement in maximum launched power by 7.5 dB. The increase in span length with 10 spans resulted in an asymmetric distribution of nonlinear power in the two halves of the transmission fiber caused less efficient MSSI, which in turn led to a reduction in Q-factor with span length. However, when the number of spans is increased at 80 km of span length, the nonlinear power asymmetry in either side of MSSI became less and less significant and resulted in an increase of the maximum transmission length by almost 83%.

In conclusion, we have demonstrated nonlinearities compensation of a 200 Gbps QPSK signal transmitted over SSMF by exploiting the FS-OPC as frequency-degenerate MSSI. We have shown that under the right set of MSSI parameters elucidated in this paper, fiber nonlinearities is significantly reduced, allowing data transmission at a 13.8 Q-factor for 3 dBm launched power over 10 × 80 km SSMF without pre or post data processing.

ORCID iDs

Abhishek Anchal https://orcid.org/0000-0003-4434-1707
Sean O'Duill https://orcid.org/0000-0002-7690-4474

References

[1] Essiambre R J and Tkach R W 2012 Capacity trends and limits of optical communication networks *Proc. IEEE* **100** 1035–55

[2] Amari A, Dobre O A, Venkatesan R, Kumar S, Ciblat P and Jaouen Y 2017 A survey on fiber nonlinearity compensation for 400 Gbps and beyond optical communication systems *IEEE Commun. Surv. Tutor.* **19** 3097–113

[3] Cisco Visual Networking Index Global Mobile Data Traffic Forecast Update 20162021 White Paper https://www.cisco.com/c/en/us/solutions/collateral/service-provider/visual-networking-index-vni/mobile-white-paper-c11-520862.html

[4] Rafique D 2016 Fiber nonlinearity compensation: commercial applications and complexity analysis *J. Lightwave Technol.* **34** 544–53

[5] Semrau D, Xu T, Shevchenko N A, Paskov M, Alvarado A, Killey R I and Bayvel P 2017 Achievable information rates estimates in optically amplified transmission systems using nonlinearity compensation and probabilistic shaping *Opt. Lett.* **42** 121–4

[6] Mizuno T, Takara H, Shibahara K, Sano A and Miyamoto Y 2016 Dense space division multiplexed transmission over multicore and multiple fiber long-haul transport systems *J. Lightwave Technol.* **34** 1484–93

[7] Essiambre R-J, Tkach R W and Ryf R 2013 Fiber nonlinearity and capacity: single-mode and multimode fibers *Optical Fiber Telecommunications VIB. Systems and Networks* (New York: Academic)

[8] Bosco G, Curri V, Carena A, Poggiolini P and Forghieri F 2011 On the performance of Nyquist-WDM terabit superchannels based on PMBPSK, PM-QPSK, PM-8QAM or PM-16QAM subcarriers *J. Lightwave Technol.* **29** 53–61

[9] Lowery A J, Du L B and Armstrong J 2007 Performance of optical OFDM in ultralong-haul WDM lightwave systems *J. Lightwave Technol.* **25** 131–8

[10] Bayvel P, Maher R, Xu T, Liga G, Shevchenko N A, Lavery D, Alvarado A and Killey R I 2016 Maximising the optical network capacity *Philos. Trans. R. Soc.* A **374** 20140440

[11] Anchal A, Kumar P and Landais P 2016 Mitigation of nonlinear effects through frequency shift free mid-span spectral inversion using counter-propagating dual pumped FWM in fiber *J. Opt.* **18** 105703

[12] Liu X, Chraplyvy A R, Winzer P J, Tkach R W and Chandrasekhar S 2013 Phase-conjugated twin waves for communication beyond the Kerr nonlinearity limit *Nat. Photon.* **7** 560–8

[13] Liang X and Kumar S 2017 Optical back propagation for fiber optic network with hybrid EDFA Raman amplification *Opt. Express* **25** 5031–43

[14] Lavery D, Ives D, Liga G, Alvarado A, Savory S J and Bayvel P 2016 The benefit of split nonlinearity compensation for single-channel optical fiber communications *IEEE Photon. Techn. Lett.* **28** 1803–6

[15] Derevyanko S A, Prilepsky J E and Turitsyn S K 2016 Capacity estimates for optical transmission based on the nonlinear Fourier transform *Nat. Comm.* **7** 12710

[16] Jansen S L, van den Borne D, Krummrich P M, Splter S, Khoe G D and de Waardt H 2006 Long-haul DWDM transmission systems employing optical phase conjugation *J. Lightwave Technol.* **25** 505–20

[17] Hu H, Jopson R M, Gnauck A H, Pilori D, Randel S and Chandrasekhar S 2016 Fiber nonlinearity compensation by repeated phase conjugation in 2.048-Tbit/s WDM transmission of PDM 16-QAM channels *2016 Optical Fiber Communications Conference and Exhibition (OFC) (Anaheim, CA)*

[18] Yariv A, Fekete D and Pepper D M 1979 Compensation for channel dispersion by nonlinear optical phase conjugation *Opt. Lett.* **4** 52–4

[19] Liang X and Kumar S 2012 Fiber nonlinearity compensation for OFDM super-channels using optical phase conjugation *Opt. Express* **20** 19921–7

[20] Xiang-Jun X X, Jian-Xin M, Qi Z, Chao-Gong D, Kui-Ru W, Chong-Xiu Y and Bo L 2009 155 Mb/s and 10 Gb/s combined FSK-IM/optical label-packet modulation signals 100 km transmission over standard single mode fiber using mid-span spectral inversion by four-wave mixing in an SOA *Chin. Phys.* B **18** 3449–52

[21] Rong H, Ayotte S, Mathlouthi W and Paniccia M M 2008 Mid-span dispersion compensation via optical phase conjugation in silicon waveguides *Optical Fiber Communication/National Fiber Optic Engineers Conf. (San Diego, CA)*

[22] Inoue K 1997 Spectral inversion with no wavelength shift based on four-wave mixing with orthogonal pump beams *Opt. Lett.* **22** 1772–4

[23] Corchia A, Antonini C, Dottavi A, Mecozzi A, Martelli F, Spano P, Guekos G and DallAra R 1999 Mid-span spectral inversion without frequency shift for fiber dispersion compensation: a system demonstration *IEEE Photon. Techno. Lett.* **11** 275–8

[24] Anchal A, Kumar P, O'Duill S, Anandarajah P M and Landais P 2016 Experimental demonstration of optical phase conjugation using counter-propagating dual pumped four-wave mixing in semiconductor optical amplifier *Opt. Comm.* **369** 106–10

[25] Houbavlis T *et al* 2005 All-optical signal processing and applications within the esprit project DO_ALL *J. Lightwave Technol.* **23** 781–801

[26] Anchal A, Kumar P and Landais P 2016 Frequency-shift free optical phase conjugation using counter-propagating dual pump four-wave mixing in fiber *J. Opt.* **18** 116–20

[27] Morshed M, Corcoran B and Lowery A J 2014 Improving broad-band mid-span spectral inversion performance for fiber nonlinearity compensation *Conf. Lasers and Electro-Optics (CLEO) - Laser Science to Photonic Applications (San Jose, CA)* pp 1–2

[28] Agrawal G P 1988 Population pulsation and nondegenerate four-wave mixing in semiconductor laser and amplifiers *J. Opt. Soc. Am.* B **5** 147–59

[29] Optilux MATLAB Toolbox https://optilux.soft112.com/

[30] Kuschnerov M, Calabro S, Piyawanno K, Spinnler B, Alfiad M S, Napoli A and Lankl B 2010 Low complexity soft differential decoding of QPSK for forward error correction in coherent optic receivers *European Conf. Optical Communication (ECOC) (Turin)* (https://doi.org/10.1109/ECOC.2010.5621498)